

41  
MTP-LVO-63-5  
May 1, 1963

43 p.

N63 21910

CODE-1

**GEORGE C. MARSHALL**

**SPACE  
FLIGHT  
CENTER**

**HUNTSVILLE, ALABAMA**

(NASA TIM X-504723) 1  
SATURN SOUND FOCUSING PREDICTION AT LOC

By

Dr. R. H. Bruns  
and

Lester F. Keene

May 1, 1963 43 p 3-4 p

OTS: \$4.60 p/h

\$1.49 ref

**OTS PRICE**

XEROX

\$

4.60 p/h

MICROFILM

\$

1.49 ref

**NASA**

GEORGE C. MARSHALL SPACE FLIGHT CENTER

---

MTP-LVO-63-5

---

SATURN SOUND FOCUSING PREDICTION AT LOC

By

Dr. R. H. Bruns  
and  
Lester F. Keene

ABSTRACT

21910

This report is an analysis of the sound pressure level distribution during Saturn launchings as a function of atmospheric conditions. Means of determining such levels are developed and conclusions relating the differing conditions between Huntsville, Alabama and Cape Canaveral are set forth.

GEORGE C. MARSHALL SPACE FLIGHT CENTER

---

MTP-LVO-63-5

---

SATURN SOUND FOCUSING

PREDICTION AT LOC

By  
Dr. R. H. Bruns and  
Lester F. Keene

ELECTRONIC ENGINEERING, MEASURING AND TRACKING OFFICE  
LAUNCH VEHICLE OPERATIONS DIVISION

## TABLE OF CONTENTS

	Page
INTRODUCTION	1
DISCUSSION	2
SUMMARY	29
APPENDIX	31
REFERENCE	39
APPROVAL	40
DISTRIBUTION	41

## LIST OF ILLUSTRATIONS

FIGURE	TITLE	PAGE
1	Sound Ray Path in a Fluid of Constant Velocity Gradient	3
2	Case 1, g Negative	5
3	Case 2, g Zero	6
4	Case 3 a, g Positive	7
5	Case 3 b, g Positive	17
6	Standard Sound Propagation Plot	12
7	Typical $H_{ij}$ , $G_{ij}$ Plot	14
8	Sound Focusing with the Launch Pad as Origin	16
9	Sound Focusing with Position s as Origin	16
10	Sound Ray Paths as Influenced by Winds	18
11	$X_{Aloft}$ as a Function of Mach Number	24
12	Y as a Function of Range	25
13	Z as a Function of Altitude	26
14	Sound Pressure Monograph	27
15	Sound Pressure Level VS Range for SA-1	34
16	Sound Pressure Level VS Range for SA-2	35
17	Sound Pressure Level VS Range for SA-3	36
18	Error Distribution, Sound Pressure Level Vs Range	37

# SYMBOL DEFINITIONS

$\theta_{oj}$	departure angle of ray j
$\theta_{ij}$	angle of ray j at altitude $h_i$
$h_i$	altitude of ith level (bottom of ith air layer)
$c_i$	sound velocity at level i
$W_i$	wind speed at level i
A	azimuth of selected vertical plane (E from N)
$A_{wi}$	direction from which wind is blowing at level i (E from N)
$W_{iA}$	wind velocity component along azimuth A
$g_i$	sound velocity gradient within layer i
$G_i$	horizontal component of sound travel within layer i
$G_{wi}$	horizontal component of air mass displacement within layer i due to wind
$G_{ij}$	ground range of ray j at altitude $H_{ij}$
$H_{ij}$	altitude of ray (j) at top of layer i
$R_i$	radius of curvature of ray path within layer i
$P_i$	pressure in millibars at level i
$AH_i$	absolute humidity at level i
$T_i$	temperature in degrees C at level i

## INTRODUCTION

Because of the high noise level generated by the Saturn engines, it is desirable to be able to determine any sound focusing situations that may occur because of meteorological conditions during the launch phase. If sound waves should be focused into a given area, grave discomfort and possibly traumata to the area's inhabitants could result. Tracking and measuring instrumentation is of a delicate nature and might suffer damage from excessive noise and vibration if in an area subject to sound focusing.

For the foregoing reasons, a procedure has been derived at LOC for determining the presence of focusing situations during the vehicle countdown. This procedure utilizes a combination of analytical and graphical methods to determine the sound ray pattern along selected azimuths from the launch pad.

In the computation of the sound ray pattern, certain simplifying assumptions are made in order to facilitate the computations:

1. Only propagation of the wave front in a vertical plane in discrete azimuths is considered, and only discrete points on the wave front are considered (this permits considering the problems in terms of ray propagation).
2. Only horizontal winds are considered.
3. The sound velocity gradient is assumed to be constant between discrete altitude levels.

## DISCUSSION

The path of a sound ray through a medium in which the velocity varies with height can be calculated by the application of Snell's law,

$$n_1 \sin \phi_1 = n_2 \sin \phi_2$$

where  $n_1$  and  $n_2$  are the indices of refraction on either side of a boundary and  $\phi_1$  and  $\phi_2$  are the angles of incidence and refraction respectively. If  $\theta_1$  and  $\theta_2$  are the angles made with the horizontal, we may write

$$n_1 \cos \theta_1 = n_2 \cos \theta_2 \text{ or}$$

$$\frac{\bar{c}}{c_1} \cos \theta_1 = \frac{\bar{c}}{c_2} \cos \theta_2$$

$\bar{c}$  being a constant reference velocity.

When the ray becomes horizontal;

$$\frac{\cos \theta}{c} = \frac{1}{c_0}$$

$c_0$  being the velocity at a height where the ray becomes horizontal.

The path of a sound ray through a layer of fluid of constant sound velocity gradient  $g$  is an arc of a circle. This follows from the fact that the curvature of a ray  $\frac{d\theta}{ds}$  is directly proportional to the velocity gradient  $\frac{dc}{dz}$ , and if the gradient is constant, then the curvature is constant. Consider the arc of a circle of radius  $R$  as shown in Figure 1.

$$\cos \theta_1 = \frac{R-d_1}{R}$$



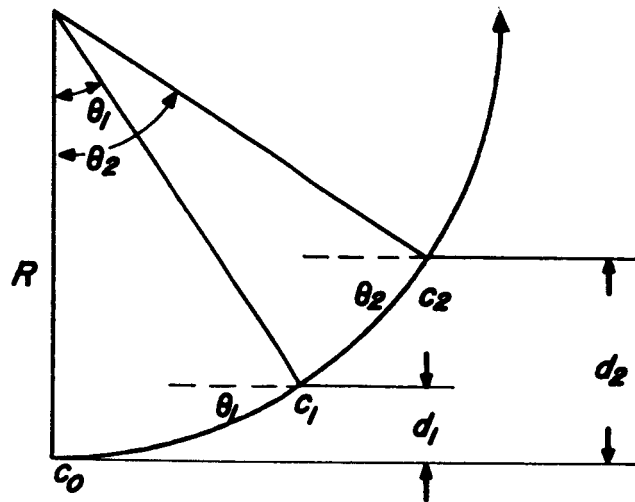


FIGURE 1  
SOUND RAY PATH IN A FLUID OF CONSTANT VELOCITY GRADIENT

$$d_1 = (1 - \cos \theta_1) R$$

$$d_2 = (1 - \cos \theta_2) R$$

$$\Delta d = d_2 - d_1 = R (\cos \theta_1 - \cos \theta_2)$$

but,

$$c_2 = c_1 + g \Delta d$$

$$\Delta d = \frac{c_2 - c_1}{g}$$

$$\frac{c_2 - c_1}{g} = R (\cos \theta_1 - \cos \theta_2)$$

From Snell's law;

$$c_2 = c_0 \cos \theta_2$$

$$c_1 = c_0 \cos \theta_1$$

$$\frac{c_0 \cos \theta_2 - c_0 \cos \theta_1}{g} = R (\cos \theta_2 - \cos \theta_1)$$

$$R = \frac{c_0}{-g}$$

$$R = \frac{c}{-g \cos \theta}$$

For the situation illustrated in Figure 1 the velocity gradient is intrinsically negative and hence R is positive. If the velocity gradient were positive, R would be negative and the path would curve downward rather than upward.

Three cases arise depending upon whether g is negative, zero, or positive.

Case 1, g negative (Fig. 2)

In the i'th layer,

$$R_i = \frac{c_i}{-g_i \cos \theta_{ij}}$$

$\cos \theta_{ij}$  being the cosine of the angle in the i'th layer for the j'th ray.

For any ray in the i'th layer,

$$\frac{\cos \theta_{ij}}{c_i} = \frac{1}{c_0} = k_j \quad (\text{constant for a given ray})$$

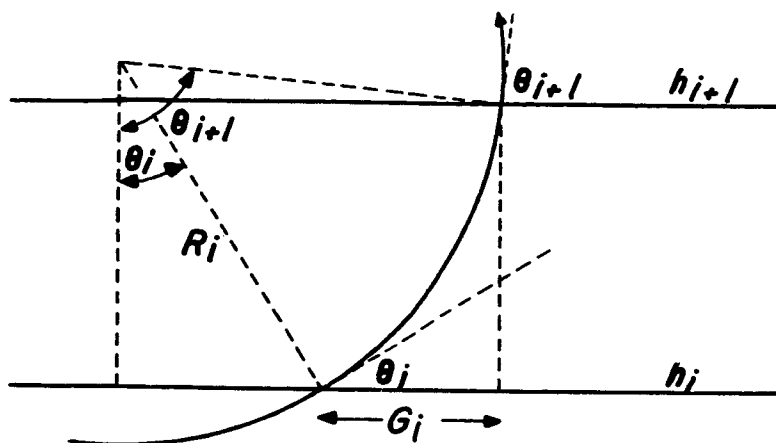


FIGURE 2  
CASE 1,  $g$  NEGATIVE

For any ray in the  $(i + 1)$  layer,

$$\frac{\cos \theta_{(i+1)j}}{c_{i+1}} = k_j$$

The horizontal component of sound travel,  $G_i$ , within level  $i$  is given by

$$G_i = R_i [\sin \theta_{(i+1)j} - \sin \theta_{ij}]$$

The altitude of ray  $j$  at the top of layer  $i$  is equal to the altitude  $h$  of the  $(i+1)$ th layer, or,

$$H_{ij} = h_{i+1}$$

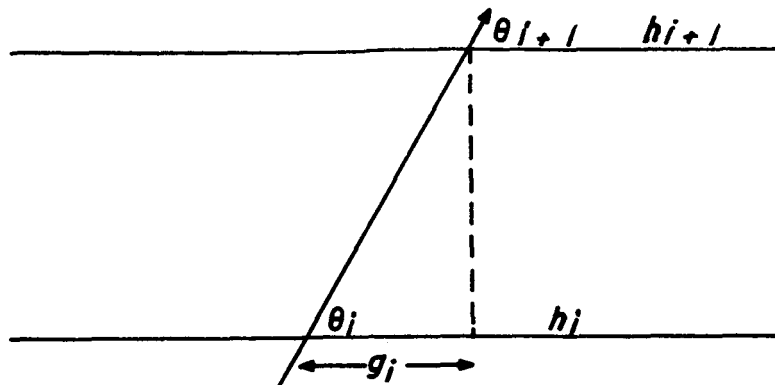


FIGURE 3  
CASE 2, g ZERO

Case 2, g zero (Fig 3)

$$\cos \theta_{(i+1)j} = \cos \theta_{ij}$$

$$G_i = (h_{i+1} - h_i) \cot \theta_{ij}$$

$$H_{ij} = h_{i+1}$$

Case 3, g positive

Under this case, there are two subcases,

$$a. \quad R_i (1 - \cos \theta_{ij}) > h_{i+1} - h_i \quad (\text{Fig. 4})$$

that is, where the ray penetrates out of the i'th layer, and,

$$b. \quad R_i (1 - \cos \theta_{ij}) < h_{i+1} - h_i \quad (\text{Fig. 5})$$

that is, where the ray reaches its maximum altitude within the i'th layer and then turns downward.

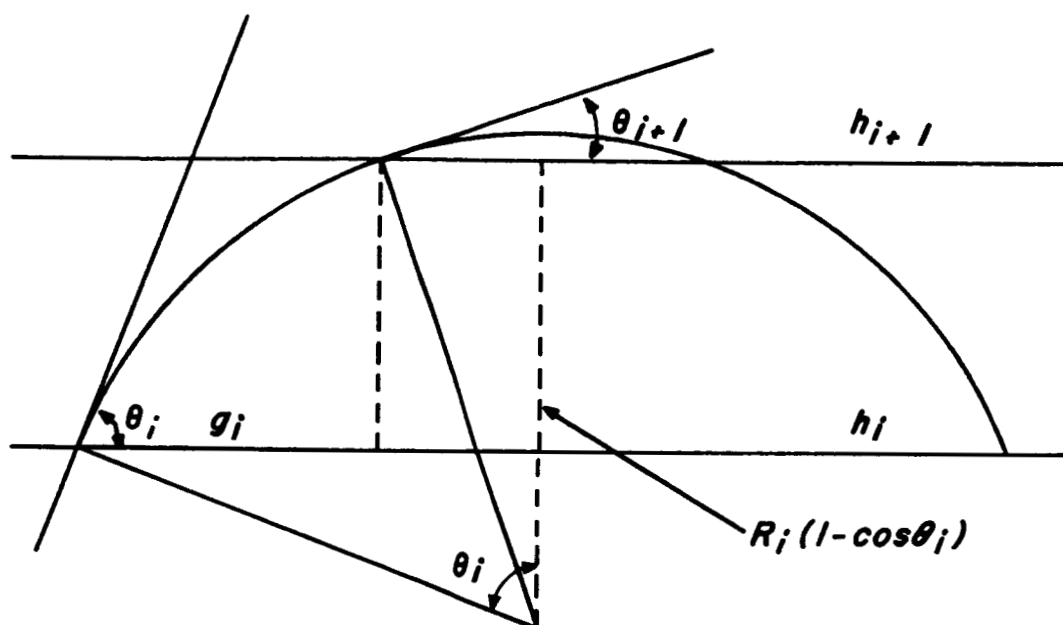


FIGURE 4  
CASE 3a,  $g$  POSITIVE

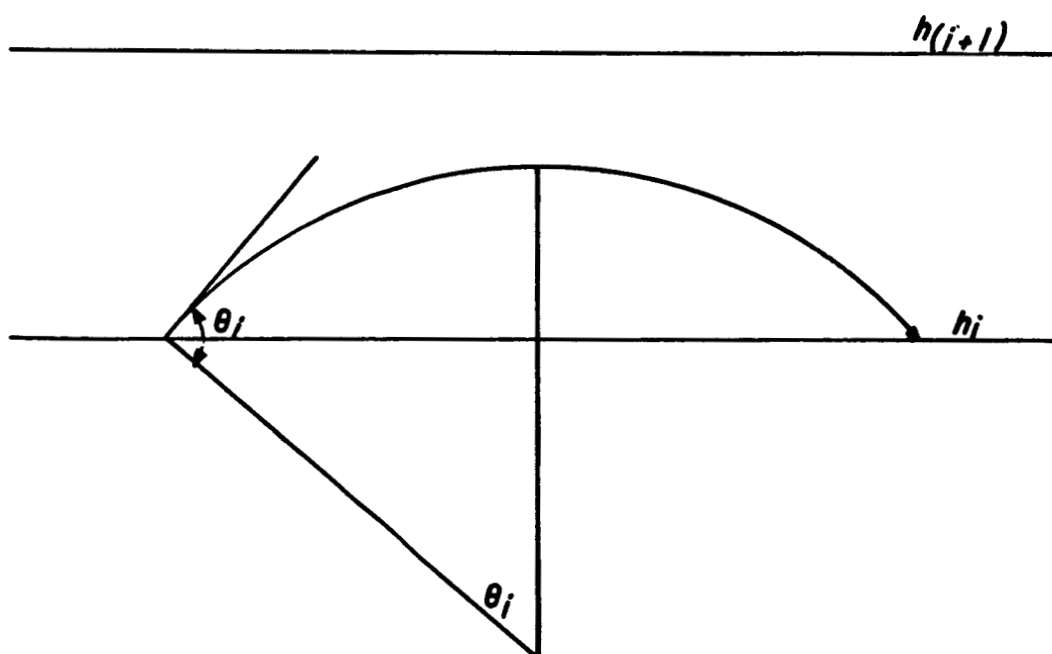


FIGURE 5  
CASE 3b,  $g$  POSITIVE

$$a. \quad R_i (1 - \cos \theta_{ij}) > h_{ij+1} - h_i$$

$$\cos \theta_{(i+1)j} = k_j \cdot c_{i+1}$$

$$G_i = R_i [\sin \theta_{ij} - \sin \theta_{(i+1)j}]$$

$$H_{ij} = h_{i+1}$$

$$b. \quad R_i (1 - \cos \theta_{ij}) < h_{i+1} - h_i$$

$$G_i = R_i \sin \theta_{ij}$$

$$H_{ij} = h_i + R_i (1 - \cos \theta_{ij})$$

For all cases, the distance traveled by the sound in the air mass is nearly

$$\sqrt{(H_{ij} - h_i)^2 + G_i^2}$$

Owing to the large radius of curvature of the sound ray in the layer, the slant distance given by the above formula closely approximates the length of the true circular path. The time for the ray to traverse the distance is found by dividing the slant distance by the average velocity in the layer.

$$t_i = \frac{2 \sqrt{(H_{ij} - h_i)^2 + G_i^2}}{c_i + c_{(i+1)}}$$

The horizontal component of air mass displacement along the azimuth line due to wind during this time is found by multiplying this time  $t_i$  by the average wind velocity component along the azimuth line in the layer.

$$G_{wi} = \left( \sqrt{(H_{ij} - h_i)^2 + G_i^2} \right) \left( \frac{W_{iA} + W_{(i+1)A}}{c_i + c_{(i+1)}} \right)$$

$$\text{where } W_{iA} = W_i \cos (A - A_{wi})$$

The ground range of the propagated ray is the sum of the distance traveled by the ray in each air mass layer, and the total air mass movement.

$$G_{ij} = \sum_0^i (G_i + G_{wi})$$

The accumulated ray path length is given by

$$P_{ij} = \sum_0^i \sqrt{(H_{ij} - h_i)^2 + (G_i + G_{wi})^2}$$

The accumulated sound travel time will be the path length divided by the average velocity of the sound ray.

$$T_{ij} = \sum_0^i \frac{2 \sqrt{(H_{ij} - h_i)^2 + (G_i + G_{wi})^2}}{c_i + c_{(i+1)}}$$

These operations have to be performed for each ray j. Typical ray departure angles defining the different rays j are:

0°	0°
2°	10°
4°	20°
6°	30°

$$H_{\max} \leq 20,000 \text{ ft.} \quad H_{\max} \leq 80,000 \text{ ft.}$$

$$10^\circ \quad 50^\circ$$

The first group of departure angles is used first to analyze the lower altitude region, in which focusing situations are most likely to occur. Only if this analysis shows a strongly disturbed ray pattern, computations are performed for the altitude region above 20,000 ft.

Rays are plotted point by point using the coordinates  $H_{ij}$  and  $G_{ij}$ , taking layers every 100 feet. The standard Rawinsonde output data are available at AMR in form of punched cards. These cards are directly used as input into the LOC sound ray computation program, providing the information on wind speed, wind direction, temperature, humidity and barometric pressure as function of altitude. The sound propagation velocity at level  $i$  is computed by:

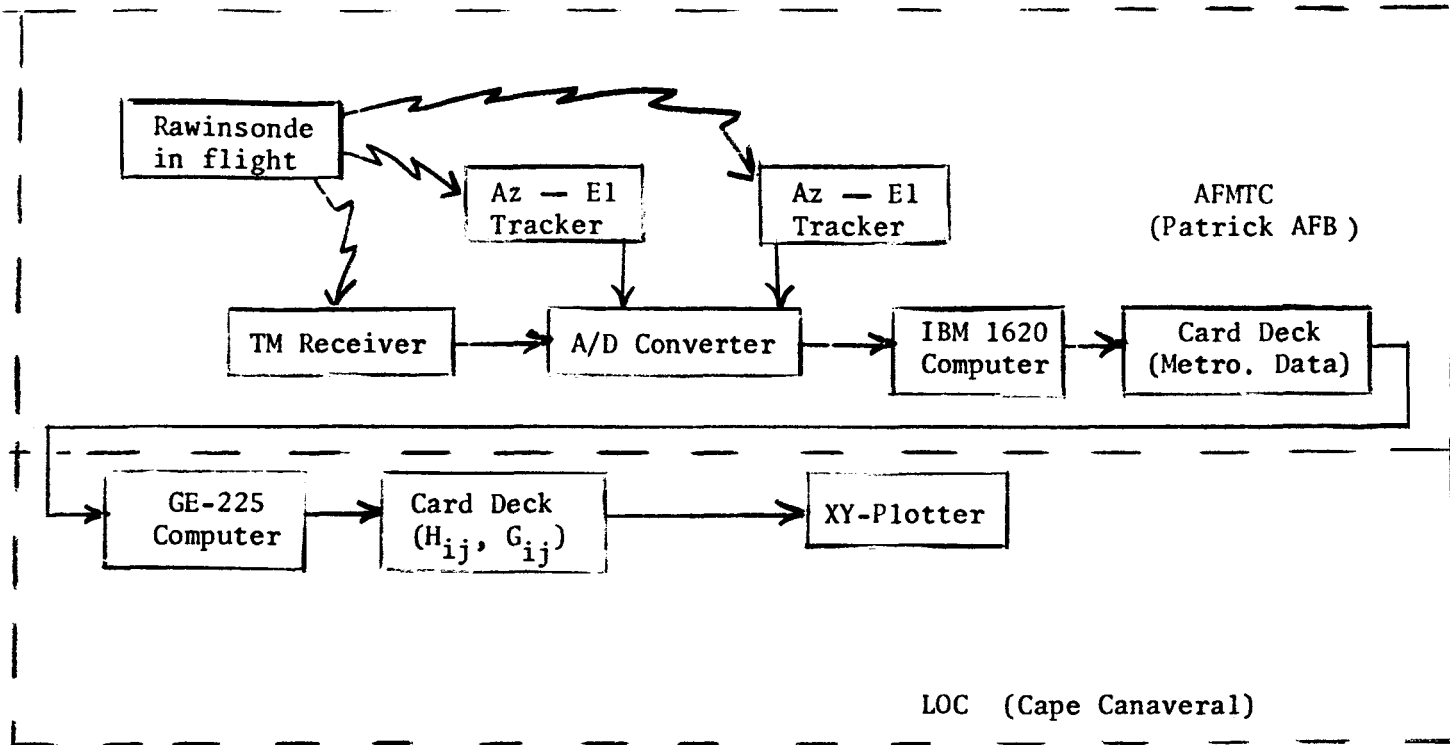
$$c_i = \left[ 65.806243 \sqrt{273.15 + T_i} \right] \cdot \left[ 1 + \frac{(273.15 + T_i) \Delta H_i}{1158.24 P_i} \right] \text{ (ft/sec)}$$

The program output consist of punched cards containing one point

$(H_{ij}, G_{ij})$  each for automatic plotting by an XY-plotter using card input.



The following diagram illustrates the data flow:



Where  $T_i$  = Air temperature [ $^{\circ}\text{C}$ ]

$AH_i$  = Absolute humidity [gram/meter<sup>3</sup>]

$P_i$  = Barometric pressure [millibars],

all values at level  $i$

The ray pattern plot so obtained is then compared with the standard sound propagation overlay (Fig. 6). This overlay in the same scale as the  $H_{ij}$ ,  $G_{ij}$  plot - has been computed under the assumption of no wind and uses the ARDC Model Atmosphere 1959 for temperature and barometric pressure data.

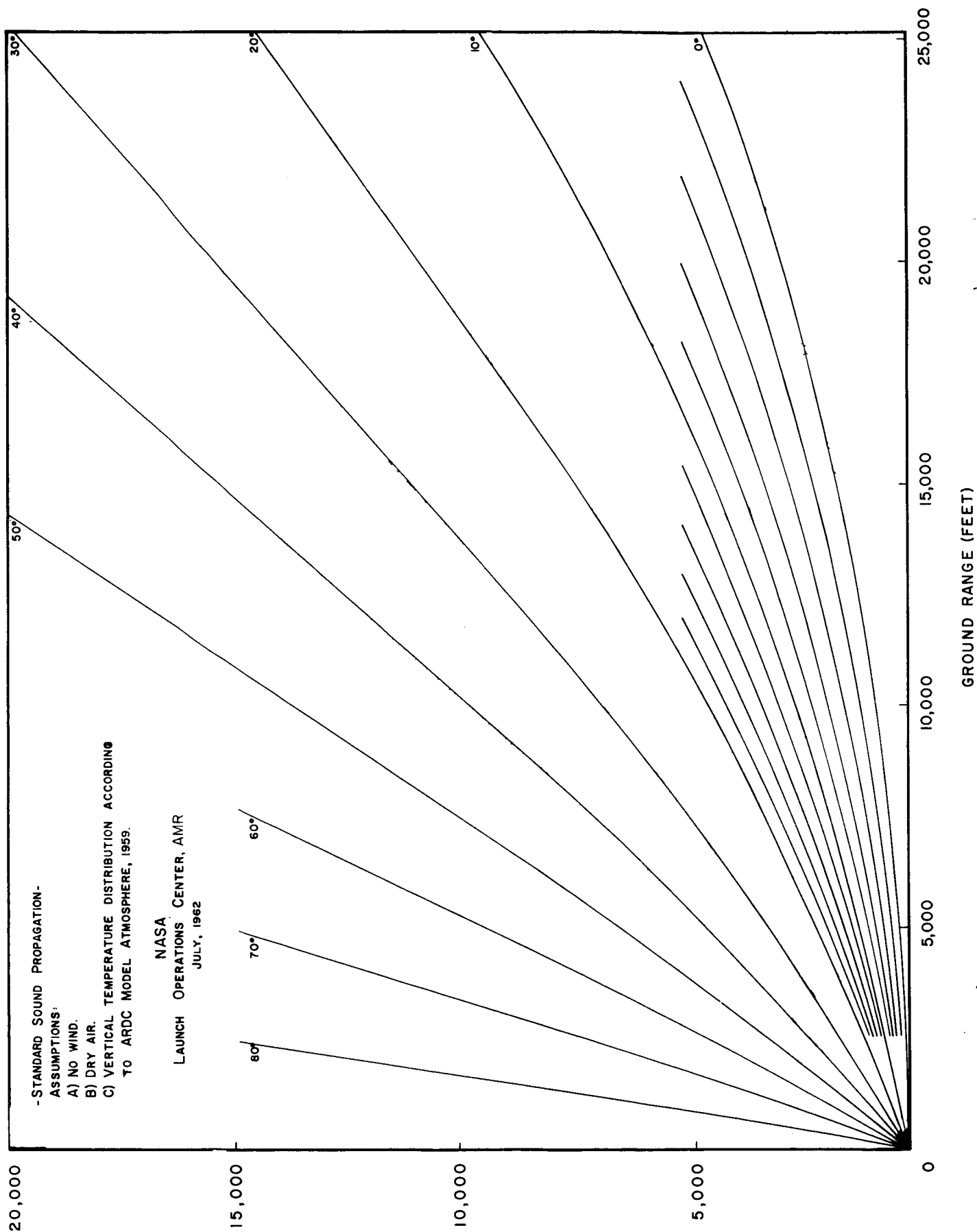
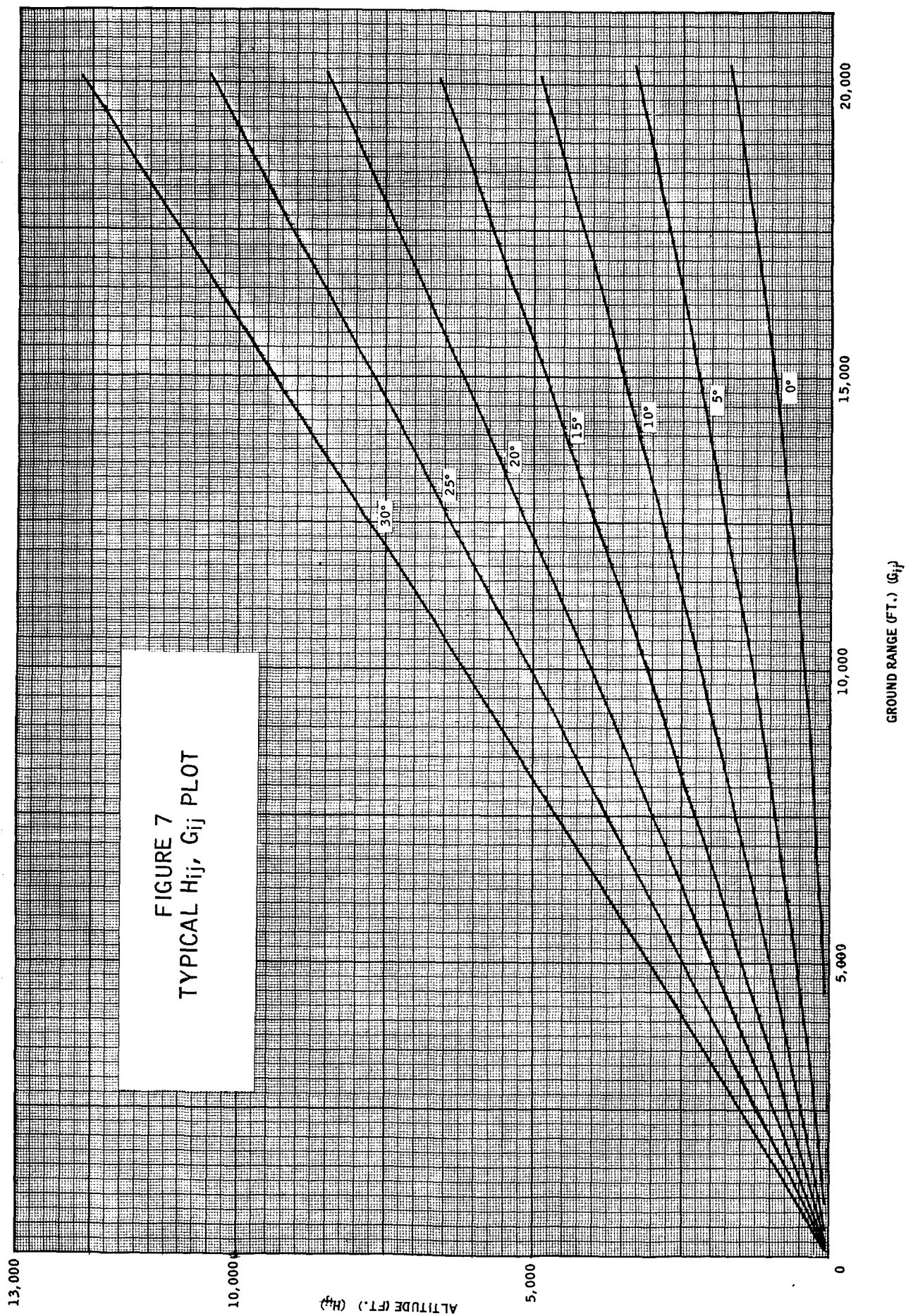


FIGURE 6  
STANDARD SOUND PROPAGATION PLOT

Typical (Attitude, Ground Range) plots are shown in Figure 7. The actual size of the plots are 40x50 centimeters scaled to correspond to 0 - 80,000 feet altitude range and 0 - 100,000 feet ground range.

The foregoing analysis assumes a vehicle on the pad, although the sound focusing problem at LOC has to deal with a vehicle in flight rather than with a stationary one. The task of a vehicle in flight seems more complicated than the analysis of a static booster firing, but it can be shown, that at least in the case of no winds, only one standard sound ray pattern computation is ever required. This case may then be utilized as a first indication of potential focusing situation for a vehicle in flight in the presence of wind.

The reciprocity of sound source and receiver in the absence of wind is first considered. We assume that a sound ray pattern has been obtained as described earlier. In the absence of wind, this pattern will have rotational symmetry about the  $h$  - axis. So far, the launch pad has been implied as origin, but the instantaneous sub-vehicle point for instance could be selected as well. In any event the computed sound ray pattern would be geometrically identical because of the absence of wind and because of the assumptions made at the outset. The following exercise will explain the underlying idea. It is assumed that the launch pad has been chosen as origin (Fig. 8). (From ref. 3). At ground distance  $G_f$  and altitude  $h_f$ , a focusing situation is detected for a vehicle with engines operating at the launch pad. The locus of focus points will be a ring at a height  $h_f$  and with a radius  $G_f$ .



This situation in itself does not seem to create a focusing condition anywhere at the ground. Let us now arbitrarily assume that the origin of our computations was at point S instead of the launch pad. The pattern so obtained (Fig. 9) would be geometrically identical with the pattern of Figure 8 and, being also symmetrical with respect to the  $h$  axis, would show that the moment the vehicle is at the altitude  $h_f$  above the launch pad, a sound focusing situation would exist for all ground points situated on a circle about the launch pad with the radius  $G_f$ .

The same reasoning applies if the launch pad is replaced by the sub-vehicle point, in the event that the vehicle has already tilted in its ascent and is not over the launch pad any more. In the absence of wind, only one set of computations is ever required to arrive at a sound ray plot that can then be used to analyze sound focusing situations for any vehicle altitude and position within the boundaries of the plot.

The reciprocity of sound source and receiver in the presence of wind is considered next. This type of analysis is only suitable for selected stations on the ground. The presence of wind makes a particular sound ray pattern computation valid only for a selected azimuth from the launch pad. In the former reciprocity case (no wind), propagation in opposite directions along the same geometric path was tacitly admitted. This being no longer acceptable, not only the origin and azimuth, but even a particular ground point within that azimuth have to be specified. Assuming the vehicle rising vertically above its launch pad (any other sub-vehicle point would require separate ray pattern computations), we have to select the ground station of interest as origin, compute the wind components in the vertical plane containing ground station and launch pad, and will eventually obtain

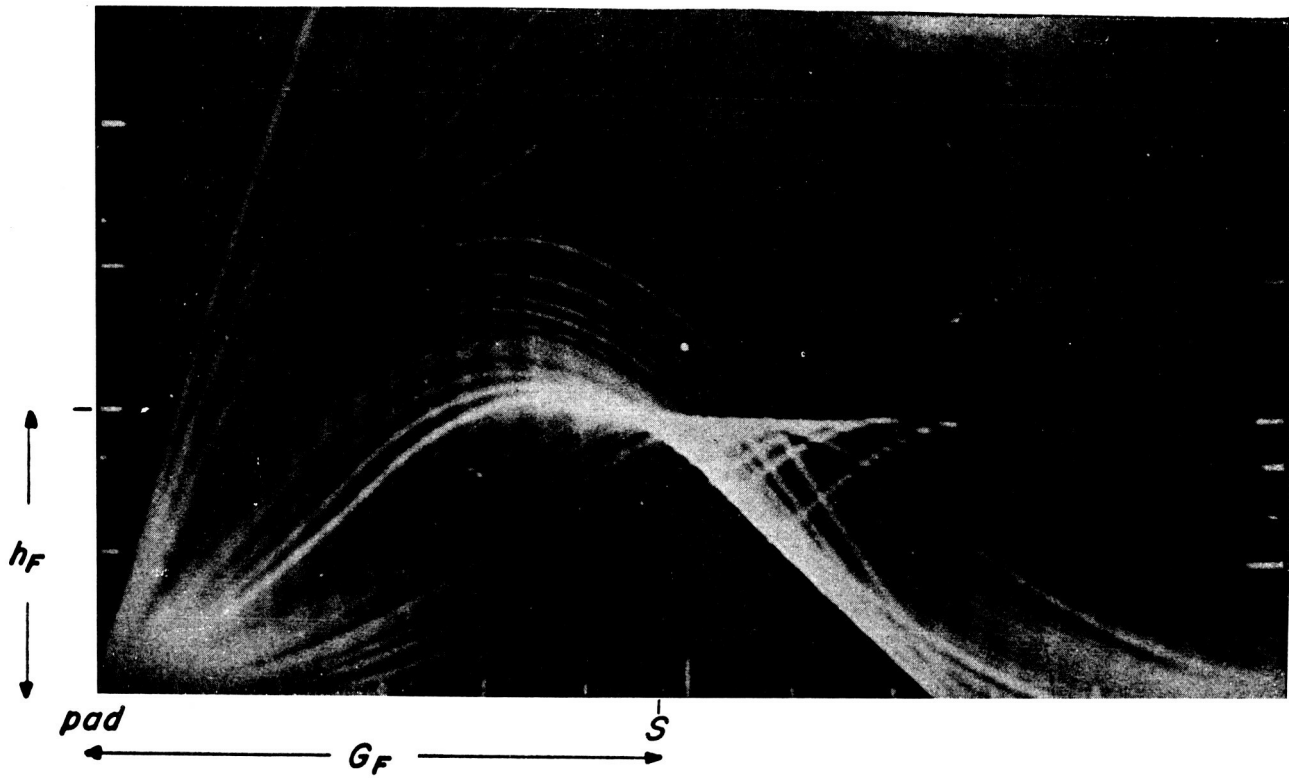


FIGURE 8  
SOUND FOCUSING WITH THE LAUNCH PAD AS ORIGIN

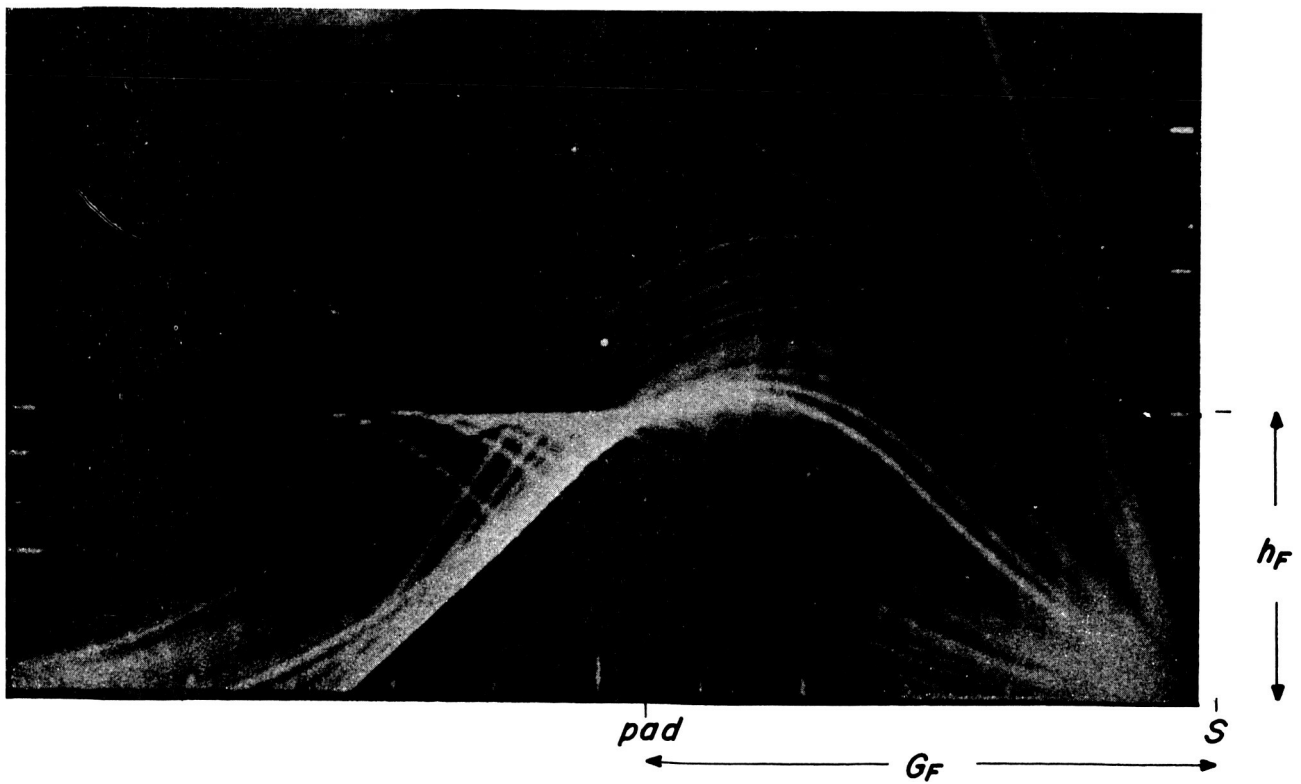


FIGURE 9  
SOUND FOCUSING WITH POSITION *S* AS ORIGIN

a sound propagation ray plot valid only for the selected ground station. This way, we have actually treated the ground station as sound source. To allow for the fact that the actual sound propagation takes place in the opposite direction, we must introduce the prevailing wind components also in the opposite direction. For proof, consider Figure 10.

A sound ray leaving the vehicle in the absence of wind would follow the path  $B'BS_1$  as it traversed the layers  $T_2$  and  $T_1$  of different indices of refraction. Conversely a ray leaving the ground station ( $S_1$ ) would traverse the path  $S_1BB'$ .

Now assume that there is wind of velocity  $w$  blowing from left to right. In this case the ray paths are not reversible, for a ray leaving the ground station will follow the path  $S_1CC'$ , and a ray leaving the vehicle at location  $C'$  will follow the path  $C'DE$ . If the sound path is to be reversed for an altitude  $H_2$ , then the direction of the wind must also be assumed to be reversed, i.e., traveling from right to left with a velocity  $-w$ . In this case, a sound ray which would have a direction of propagation  $S_1B$  with no wind and a direction  $S_1C$  with the actual wind would have a direction  $S_1A$  under the assumed wind conditions and would intersect the vehicle at  $A'$ .

Note that the rays  $S_1AA'$  and  $C'DE$  are geometrically identical, but have an opposite sense of propagation. It is therefore possible to superimpose the two rays at  $S_1$  with the result that identical ray geometry will be achieved for a computed ray  $S_1AA'$  (assuming wind  $-w$ ) and for the actual sound propagation ray under wind  $w$  and with the vehicle at  $A'$  (In the absence of wind the ray from  $A'$  would be parallel to  $B'BS$ .)

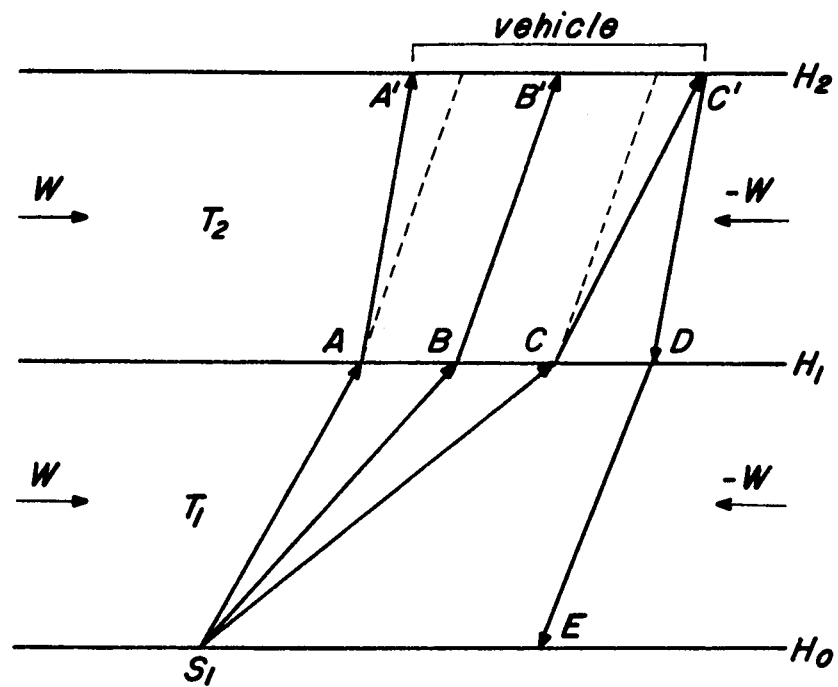


FIGURE 10  
SOUND RAY PATHS AS INFLUENCED BY WINDS



We will now discuss the significance of the sound focusing problem at Cape Canaveral. During full time static firings of the Saturn booster at George C. Marshall Space Flight Center, significant differences in sound intensity were noted in the surrounding areas on various days. An intensive sound analysis program is being conducted at MSFC with emphasis on the effects to be expected in the Huntsville urban area. The situation in the Cape Canaveral area is different in several respects. First, the meteorological conditions that favor sound focusing are mainly pronounced temperature inversions. Northern Alabama experiences this condition much more frequently than Central Florida. Second, the topographic conditions at Huntsville tend to further disturb the air layer structure especially in connection with winds and may even cause echo effects, while the flat terrain around Cape Canaveral has neither effect. But most of all, the sound field effects a stationary vehicle creates are much more severe than those created by a flight vehicle. In case of sound focusing, source (vehicle) and receiver occupy corresponding focus points (Figures 8 and 9). The essential difference between a stationary and flight vehicle is that the stationary vehicle remains at its focus point indefinitely, while the flight vehicle passes only through its focus point within a fraction of a second, thereby creating abnormal sound intensity at the ground just for that short interval. The only exception is the lift-off phase, during which the engines operate for several seconds at the launch pad. Again, the effect would last only for seconds as opposed to several minutes in case of a static firing.

As the vehicle gains altitude, several factors influence the sound intensity being received on the ground.

Barring upper air focusing conditions, the sound pressure levels caused by a flying vehicle will be always smaller than those produced by the same vehicle standing with operating engines on the launch pad. To investigate the entire situation, one may utilize the general expression for the sound pressure level.

$$\text{SPL} = \text{PWL} - 10 (1 + \log A) - 20 \log |r| - 10 \log \frac{400}{\rho_o c} \quad [\text{db}]$$

where

PWL The power level of the sound source in db, referenced to

a power of  $10^{-13}$  watts.  $(\text{PWL} = 10 \log \frac{P_1}{10^{-13}})$

A The part of a spherical surface in steradians through which sound is propagated. The assumed sphere has unit radius and is centered around the sound source.

For instance:

$A = 4\pi$  for spherical propagation

$A = 2\pi$  for hemispherical propagation

r Distance between sound source and the point in meters, where SPL is experienced (receiver).

$\rho_o$  The air density in  $\text{kg-m}^{-3}$  at the sound source.

c The sound velocity in  $\text{m-sec}^{-1}$  at the sound source.

Assuming the following identities,

$$X = -10 (1 + \log A)$$

$$Y = -20 \log |r|$$

$$Z = -10 \log \frac{400}{\rho_o c}$$

the formula for the sound pressure level can be simplified to

$$\text{SPL} = \text{PWL} + X + Y + Z \text{ [db]}$$

To begin the discussion with the source power level, PWL, a typical value for a Saturn S-I booster having 1.3 million pounds of thrust is 207 db with a standard error of  $\pm 8.1$  db. This value is based on a total of 17 observations during SA-1, 2 and 3 launchings. See appendix A. Sound observations beyond 5000 meters distance from the launch pad were discarded because they show clearly systematic influences of meteorological conditions on the sound propagation. Based on this empirically obtained power level, the following equation can be used to predict other power levels:

$$\text{PWL} = 207 + 10 \log \frac{F}{1.3} \text{ [db]}$$

where

$F$  = Thrust of stage in  $10^6$  lbs.

As a vehicle gains altitude, thrust will increase above the value at sea level. In the case of the Saturn S-I stage, this increase causes nearly 1 db rise in power level during the latter part of powered flight. A 3 db drop of power level is experienced from thrust termination of the four S-I inner engines. The following table of events will illustrate the S-I power level behavior.

Event	PWL
Lift-off	207 db
Prior to inner engine cutoff	208 db
After inner engine cutoff	205 db

The next term in the sound pressure equation:

$$X = -10 (1 + \log A) \quad [\text{db}]$$

contributes to the sound pressure level in a more complicated way. As long as the vehicle occupies the launch stand, semispherical sound propagation takes place so that:

$$\begin{array}{lcl} A & = & 2\pi \text{ and } X = -10 (1 + \log 2\pi) = -18 \text{ db} \\ \text{ground} & & \text{ground} \end{array}$$

In flight, spherical sound propagation leads to a value

$$\begin{array}{lcl} A & = & 4\pi \text{ and } X = -10 (1 + \log 4\pi) = -21 \text{ db} \\ \text{aloft} & & \text{aloft} \end{array}$$

This latter condition prevails only as long as the vehicle has not yet reached Mach number one. Once this happens, the area  $A$  of sound propagation depends solely on the Mach number  $M$ , that is to say, the Mach angle  $\alpha$ . This angle is defined as

$$\alpha = \arcsin \frac{1}{M} \quad \text{for } M \geq 1$$

Sound will propagate only within the cone defined by the vehicle axis (more strictly by the direction of the vehicle velocity vector) and the cone angle  $2\alpha$ . Such an angle produces on the unit sphere the area

$$A = 4\pi \sin^2 \frac{\alpha}{2} \quad [\text{sterad}]$$

so that the  $X$ -value aloft finally becomes

$$\begin{aligned} x_{\text{aloft}} &= -10 (1 + \log 4\pi \sin^2 \frac{\alpha}{2}) \quad \text{for } M \geq 1 \\ &= -10 (1 + \log 4\pi) = -21 \text{ db} \quad \text{for } M < 1 \end{aligned}$$

The confinement of the total sound energy to a cone means an increased contribution of the X-value to the sound pressure level with increasing Mach number. Numerical values can be obtained from the attached X-graph (Fig. 11). Sound originated after the vehicle reaches Mach number one will only be observed by ground stations situated inside the prevailing "2 $\alpha$  Mach-cone".

The following term

$$Y = -20 \log |r| \quad [\text{db}]$$

in the equation for sound pressure level depends only on the distance of the sound receiver from the sound source. This term accounts for the rapid sound pressure decrease observed on the ground as the vehicle ascends. Values for Y can be obtained from the attached Y-graph (Fig. 12).

The last term

$$Z = 10 \log \frac{400}{\rho_o c} \quad [\text{db}]$$

is a function of air density and the sound velocity, both as prevailing at the sound source. Using a standard atmosphere model, Z may be expressed as function of sound source altitude, as has been done in the attached Z-graph (Fig. 13). The constant value 400 produces a nearly zero value for Z at sea level.

As an aid to the prediction of sound pressure levels, a nomograph has been constructed showing the functional dependence of the sound pressure level (SPL) on the power level (PWL) of the source and the distance from the source (Fig. 14). The SPL reference was taken to be  $2 \times 10^{-5}$  newtons per square meter (0.0002 microbar) and the PWL reference was taken to be  $10^{-13}$  watts. The nomograph is used by laying a straight edge connecting the known values on any two of the scales and reading the unknown from the third scale.

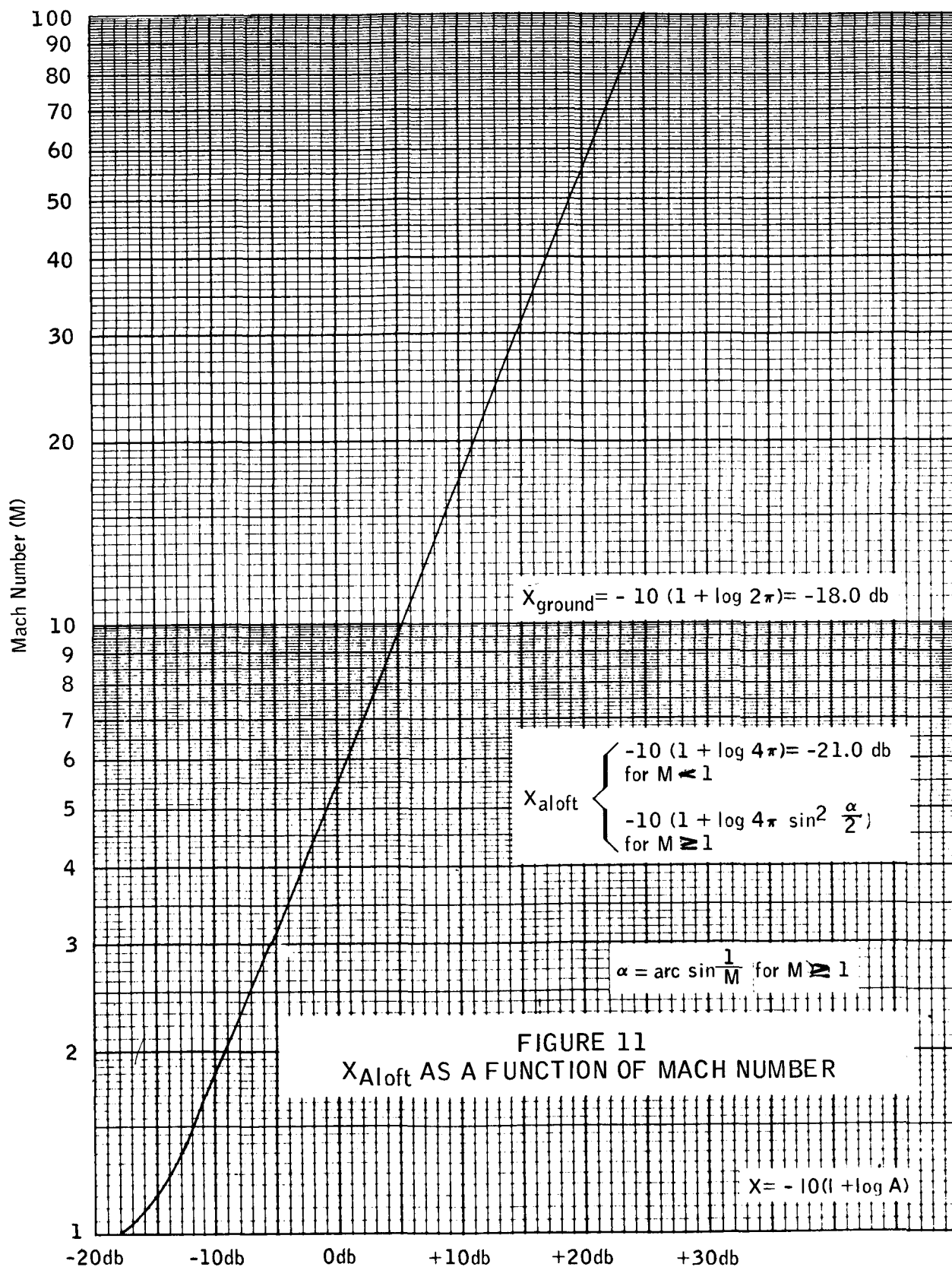
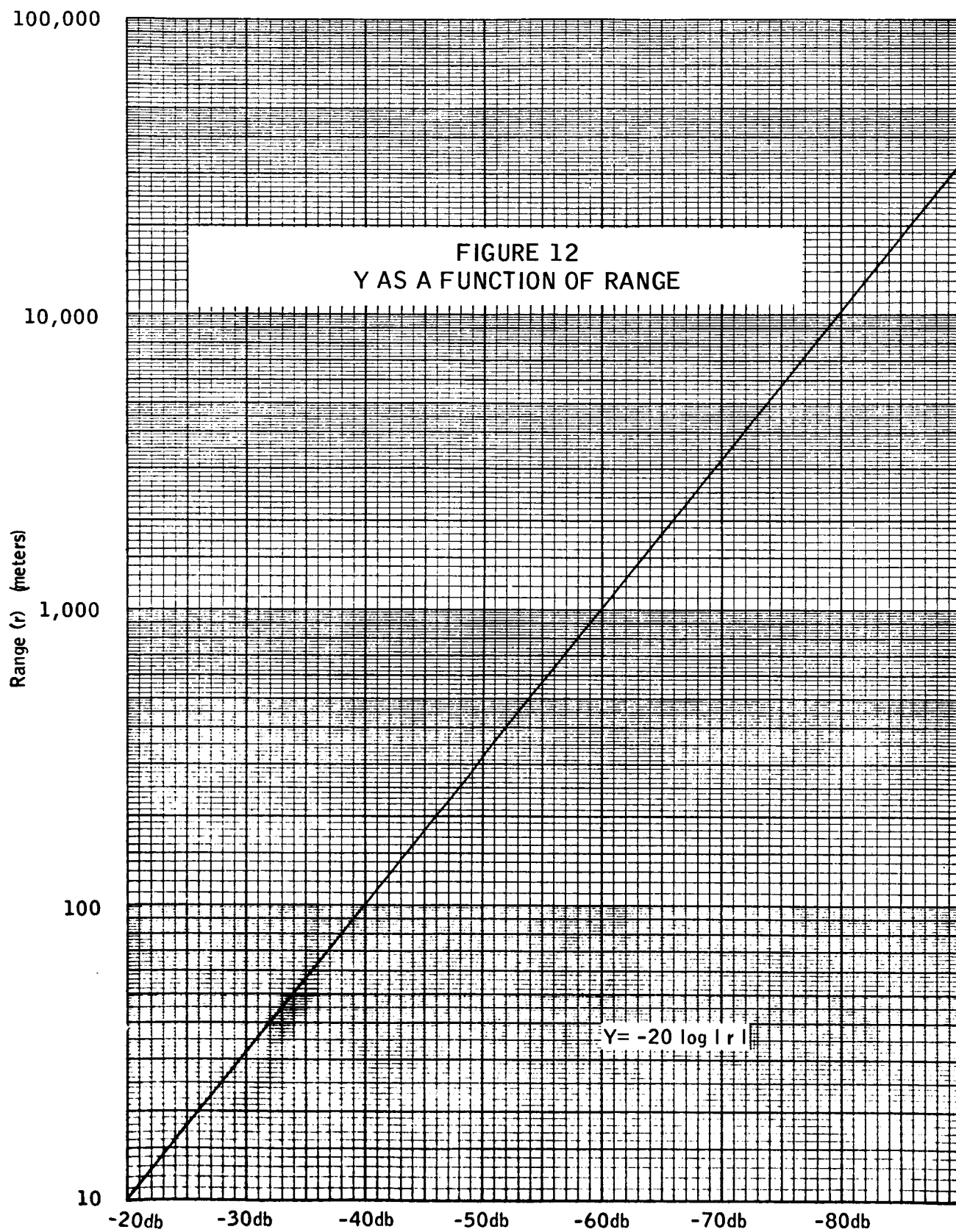
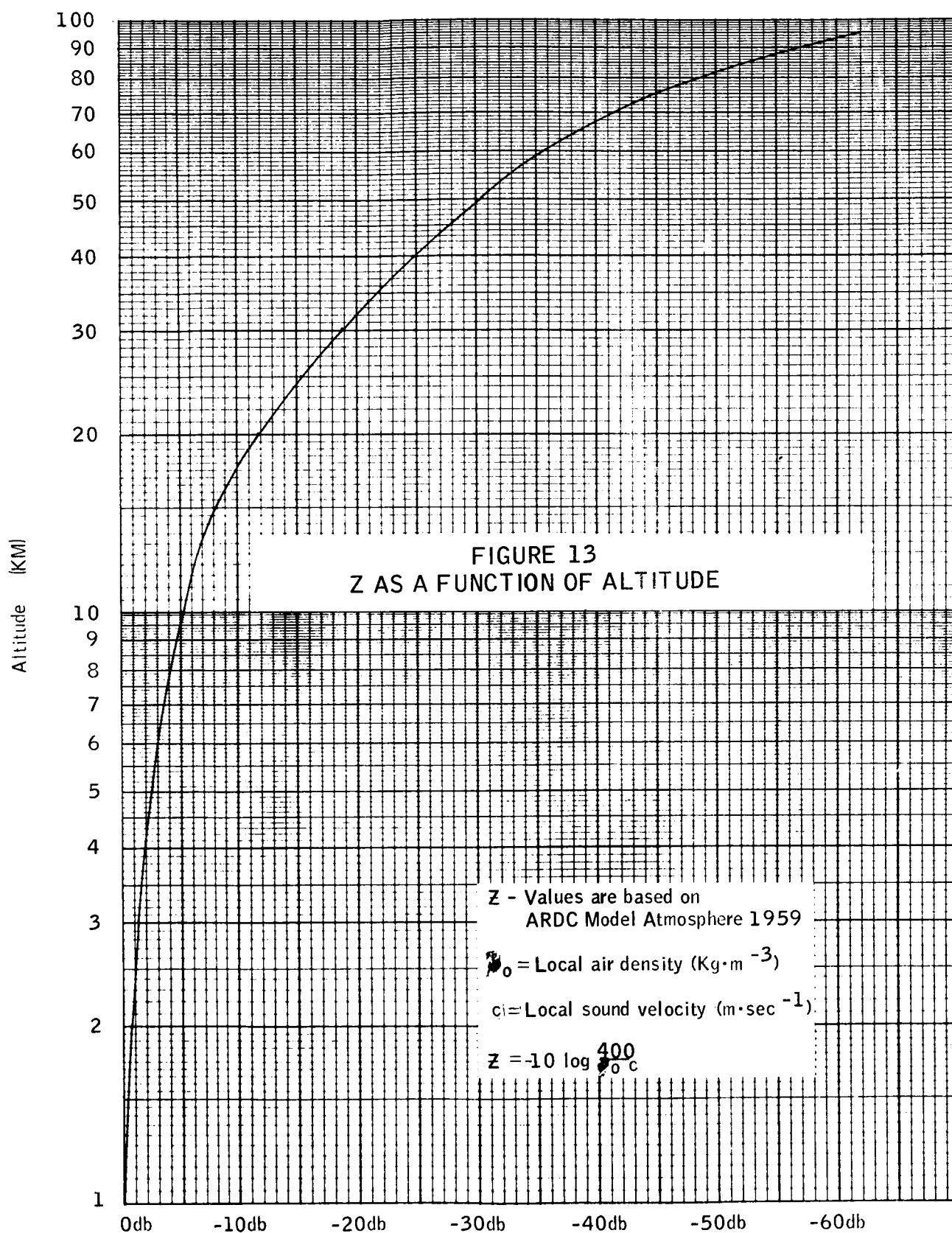
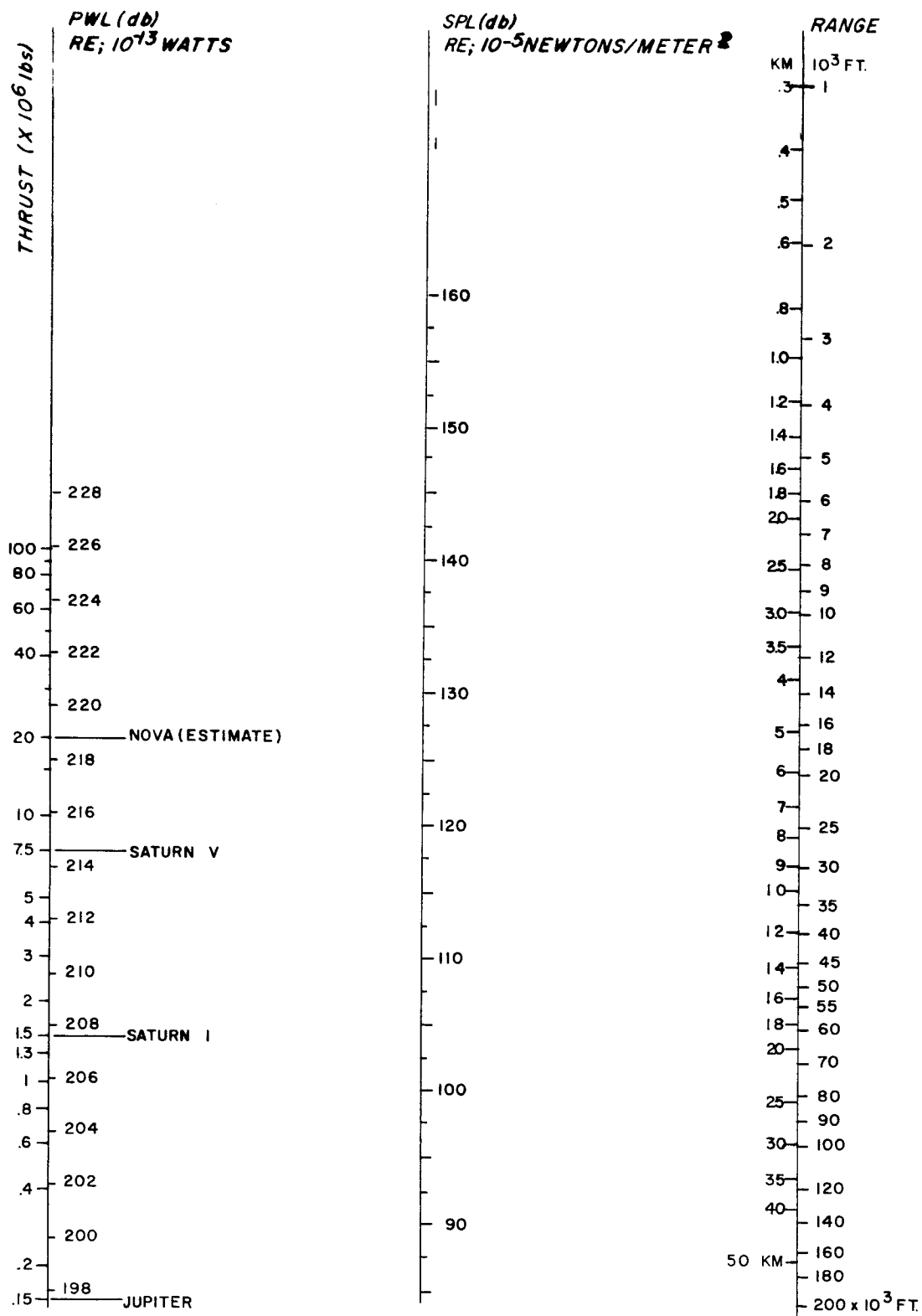


FIGURE 11  
 $X_{Aloft}$  AS A FUNCTION OF MACH NUMBER









M-LVO-EF JAN. 1963

FIGURE 14  
SOUND PRESSURE MONOGRAPH

## SUMMARY

A relatively simple method has been developed for predicting sound ray focusing, both with wind and under no wind conditions. In the case of no wind, only one standard sound ray pattern is required. An analysis of actual sound measurement data of SA-1, SA-2, and SA-3 launching has shown that the normal sound pressure level at points on the ground follows the theoretical law, (see appendix).

$$\text{SPL} = \text{PWL} - 18 - C \log |r|$$

where

$$\text{PWL} = 206.5 \pm 8.1 \text{ db}$$

$$C = 19.6 \pm 2.0$$

$r$  = range in meters

In actual use of this equation, PWL is taken to be 207, and  $C$  is taken to be 20.

## APPENDIX

The value of 207 db corresponding to the Saturn C-1 booster thrust of 1.3 million pounds was obtained by an analysis of sound level measurements made on SA-1, SA-2, and SA-3. (Refs 1 and 2) A least squares adjustment of the data was performed to arrive at the most probable value.

The tabulated values of the range and the measured SPL's are shown below:

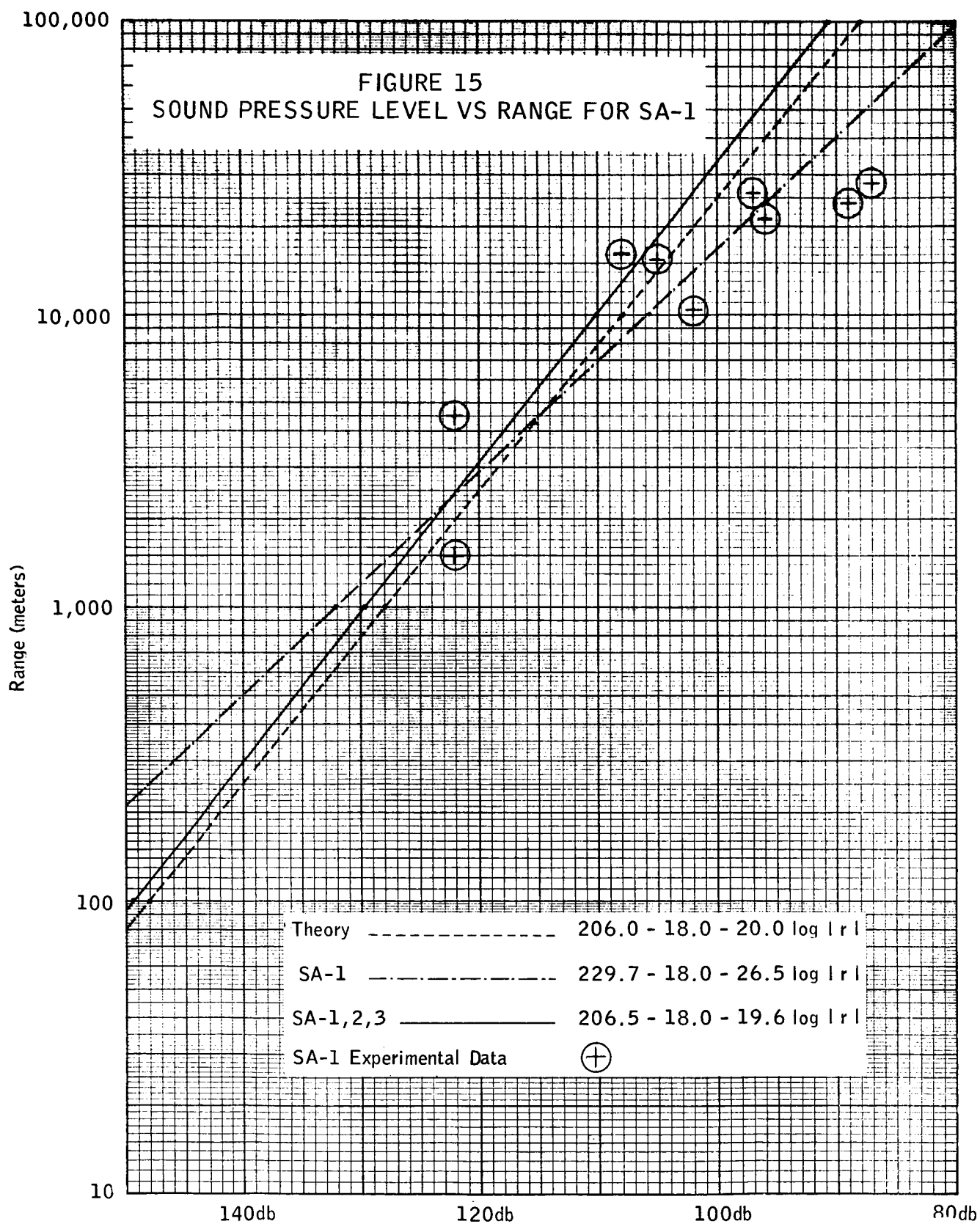
Vehicle	Range meters	SPL db
SA-1 (Figure 15)	1524	122
	4505	122
	10302	102
	15773	105*
	16551	108*
	22037	96*
	24262	89*
	26441	97*
SA-2 (Figure 16)	28000	87*
	301	137
	1524	126
	4294	112*
	4505	122*
	7523	113*
	9022	124*
	10302	112*

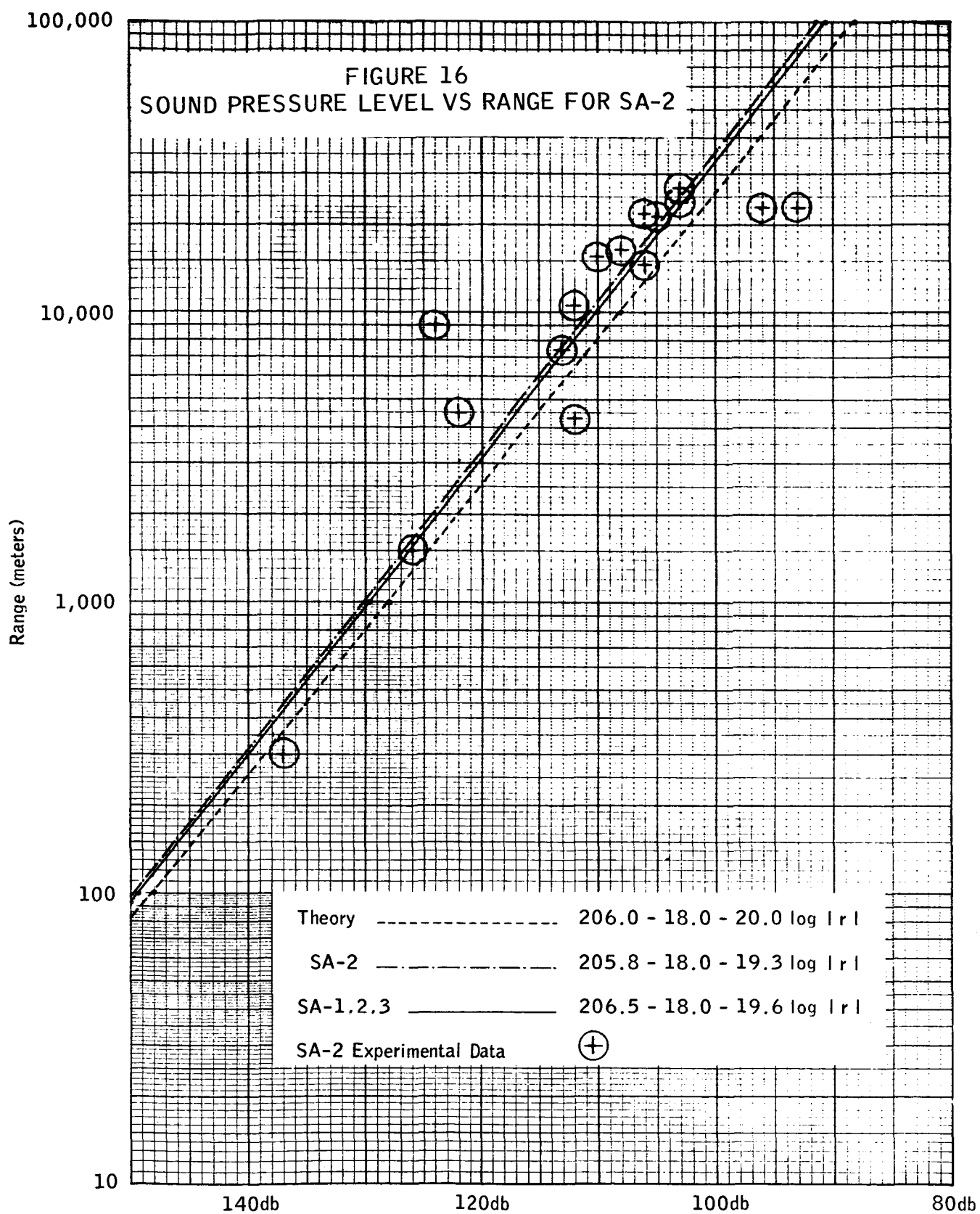
Vehicle	Range meters	SPL db
SA-2	14794	106*
	15773	110*
	16551	108*
	21717	105*
	22037	106*
	22877	96*
	23379	93*
	24262	103*
	26441	103*
SA-3 (Figure 17)	45	153
	60	150
	183	148
	366	140
	1524	124
	4294	116
	4511	117
	7523	115
	9022	112
	10302	112
	14794	104
	15574	105
	21717	109
	22877	108
	23379	105
	24262	111
	26441	100

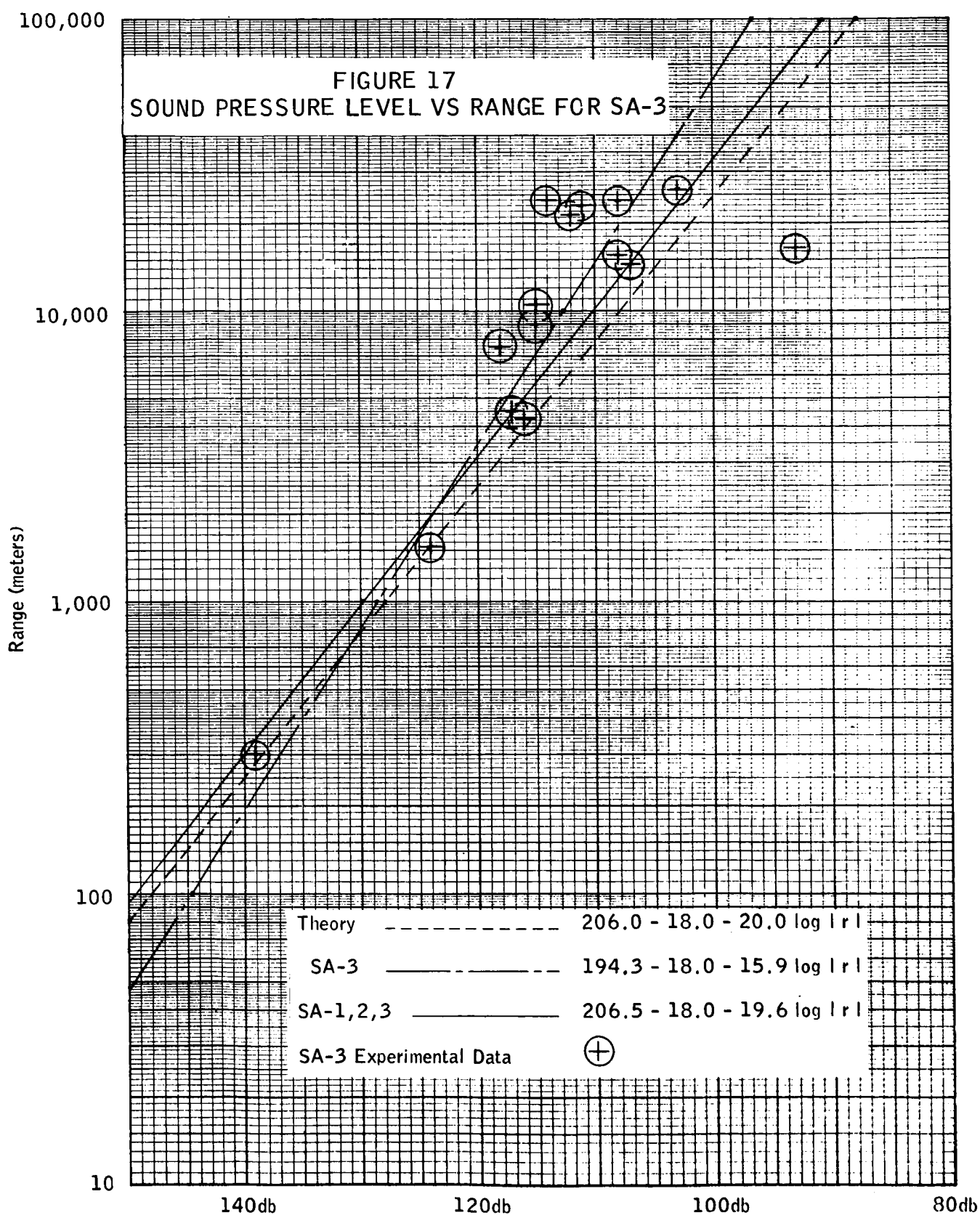
The values marked with an asterisk have been corrected by having 3db subtracted from the observed values to take into account spherical instead of hemispherical propagation. At the time of firing, meteorological conditions were such that even the horizontal sound rays originating from the vehicle on the pad were refracted upwards. Therefore no sound waves propagated along the ground surface reached the locations in question, and the sound pressure levels recorded there were due to the rays originating from the vehicle in flight. Therefore, the sound waves traveling through the air and spreading out spherically (not constrained along the surface of the earth) would be subjected to spherical instead of hemispherical divergence. For this reason, the factor  $4\pi$  instead of  $2\pi$  would have to be used in the SPL equation.

(Page 23 )

In Figures 15, 16, and 17 are shown the SPL vs range curve for SA-1, SA-2, and SA-3. The value of the PWL used in the curve marked theory was a predicted value from reference 4. The standard deviation of the final value of PWL from the three vehicles was  $\pm 8.1$  db. The standard deviation in the coefficient of  $\log |r|$  was  $\pm 2.0$  db. An error plot of the function  $(206.5 \pm 8.1) - 18.0 - (19.6 \pm 2.0) \log |r|$  is shown in Figure 18. with the center line being the most probable value of the function, and the two limit lines, the  $1\sigma$  values of the deviations.









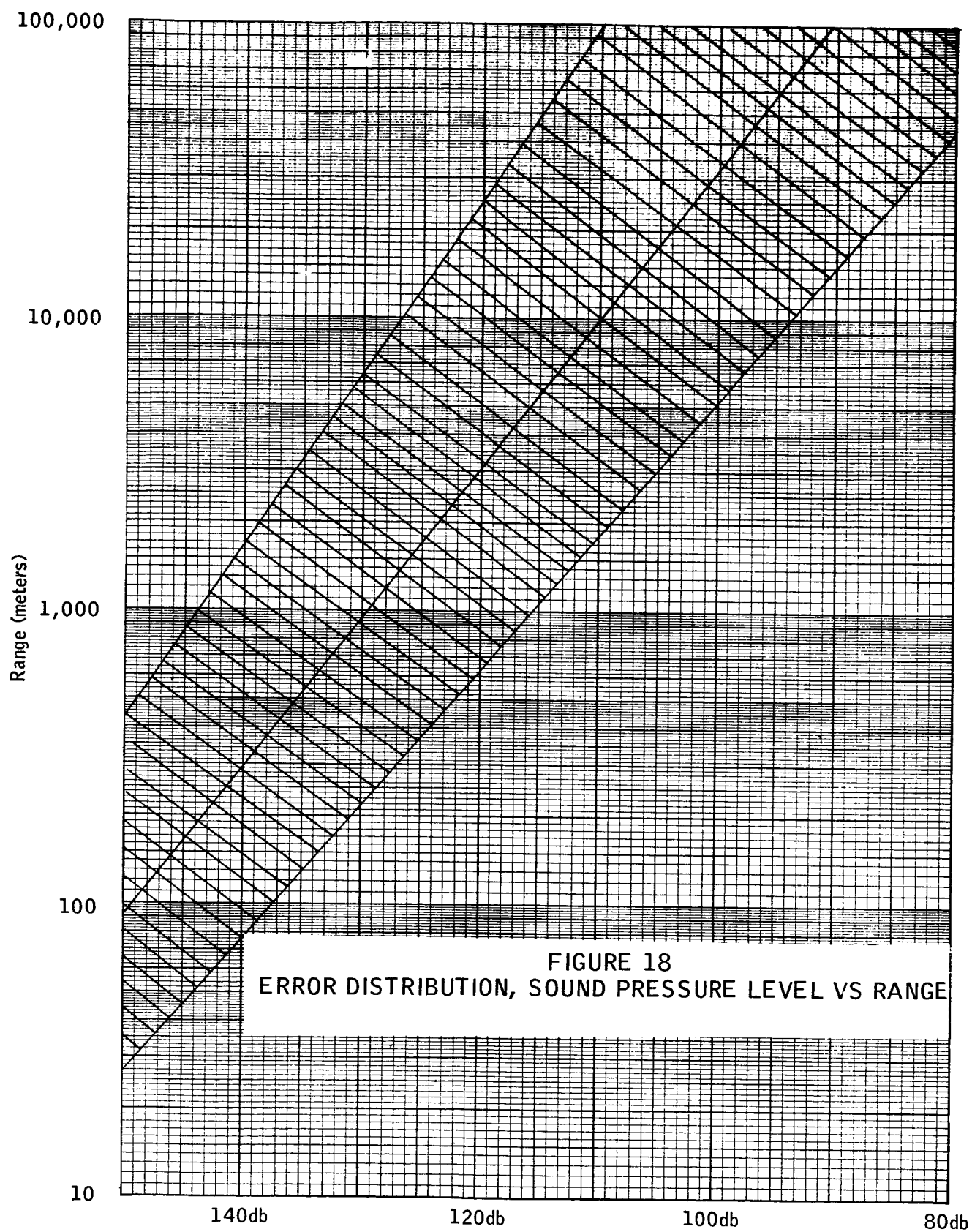


FIGURE 18  
ERROR DISTRIBUTION, SOUND PRESSURE LEVEL VS RANGE

## REFERENCES

1. Coleman, D.J.: Results of NASA-LOD Sound Pressure Level Measurements During SA-2 Launch, NASA-MSFC report, MTP-LOD-62-9, May 21, 1962.
2. Byrne, F. and Crowell, J.: Preliminary Results of LVO Sound Pressure Level Measurements During SA-3 Launch, NASA-LOC report, Instrumentation Planning Office, Launch Operations Center, November 28, 1962.
3. Perkins, B., Lorrain, P.H., and Townsend, W.H.: Forecasting the Focus of Air Blasts Due to Meteorological Conditions in the Lower Atmosphere, U.S. Army Ballistic Research Laboratories, Report #1118, October 1960.

APPROVAL

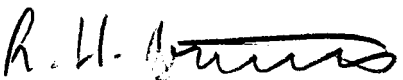
MTP-LVO-63-5

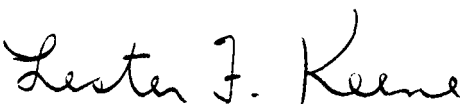
## SATURN SOUND FOCUSING PREDICTION AT LOC

By

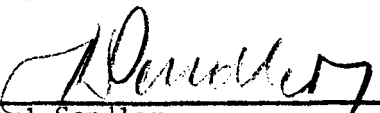
DR. R. H. Bruns  
and  
Lester F. Keene

## ORIGINATORS:

  
\_\_\_\_\_  
Dr. R. H. Bruns  
Chief, Flight Instrumentation  
Planning and Analysis Group

  
\_\_\_\_\_  
Lester F. Keene  
Deputy Chief, Flight Instrumentation  
Planning and Analysis Group

## APPROVAL:

  
\_\_\_\_\_  
Karl Sendler  
Chief, Electronic Engineering,  
Measuring and Tracking Office

The information in this report has been reviewed for security classification. Review of any information concerning Department of Defense or Atomic Energy Commission programs has been made by the MSFC Security Classification Officer. This report, in its entirety, has been determined to be unclassified.

## DISTRIBUTION

		Copies
M-DIR		1
M-AERO	Attn: Dr. Geissler	1
M-AERO-G	Attn: Mr. O. E. Smith	1
M-COMP-R		1
M-LVO-E	Attn: Mr. Sendler	1
M-LVO-EF	Attn: Dr. Bruns (3)	3
M-LVO-ED	Data Office	1
M-LVO-EM	Attn: Mr. Wilkinson	1
M-LVO-EM	Attn: Mr. Jones	1
M-LVO-EP	Attn: Mr. Collins	1
M-MS-IP	Attn: I. Remer	1
M-MS-IPL	Attn: Lois Robertson	1
M-P&VE	Attn: Mr. Mrazek	1
M-P&VE	Attn: Mr. Wilhold	1
M-RP-P	Attn: Mr. Hembree	1
M-TEST	Attn: Mr. Thornton	1
LO-DIR		1
LO-H	Attn: Lt. Col Petrone	1
LO-JRL	Technical Library	5
LO-JRT	Attn: Mr. R. Hill	1
LO-K	Attn: Mr. King	1
LO-N	Attn: Mr. Taiani	1
LO-TS	Attn: Dr. Knothe	1
NASA HEADQUARTERS, MLO	Attn: Mr. D. Schwartz	1
SCIENTIFIC AND TECHNICAL INFORMATION FACILITY		
P. O. BOX 5700		
BETHESDA, MARYLAND,	Attn: S-AK/RKT, NASA Representative	2
Total Number of Copies		32

N63-21910

Case file

December 10, 1963

ERRATA

GEORGE C. MARSHALL SPACE FLIGHT CENTER

---

MTP-LV0-63-5

---

SATURN SOUND FOCUSING PREDICTION AT LOC

By

Dr. R. H. Bruns

and

Lester F. Keene

dated

May 1, 1963

Page 27, Figure 14: Change from

SPL(db)

RE;  $10^{-5}$  NEWTONS/METER<sup>2</sup>

to read

SPL(db)

RE;  $2 \times 10^{-5}$  NEWTONS/METER<sup>2</sup>